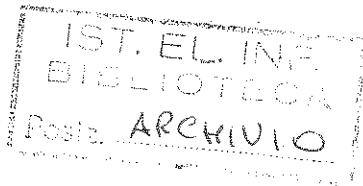


ISRAMT' 99

A2-21
(1999)



1999 7th International Symposium on Recent Advances in Microwave Technology Proceedings

Edited by

C. Camacho Peñalosa
B. S. Rawat

Organized by

Universidad de Málaga, Spain
University of Nevada, USA

Málaga (Spain), 13-17 December 1999

© ISRAMT' 99

The organising committee do not hold any responsibility for the statements made or opinions expressed in the papers included in this volume. The editors assume no responsibility for the accuracy, completeness or usefulness of the information disclosed in this volume.

This book or any part thereof may not be reproduced in any form without the written permission of the publisher.

All rights reserved. No part of this Publication may be reproduced, stored in a retrieval system or transmitted in any form or by any means: electronic, electrostatic, magnetic tape, mechanical, photocopying, recording or otherwise, without permission in writing from the Publishers.

This book has been reproduced from the best available copy.

First Edition 1999

1999 7th International Symposium on Recent Advances in Microwave Technology

Edita: Centro de Ediciones de la Diputación
Provincial de Málaga (CEDMA)

I.S.B.N. 84 7785 349 5

Depósito Legal: MA 1025/99

Impreso en España – Printed in Spain

PERFORMANCE OF A BORN-APPROXIMATION MICROWAVE TOMOGRAPHIC TECHNIQUE UNDER NON-BORN CONDITIONS

R2

Emanuele Salerno
Consiglio Nazionale delle Ricerche - IEI
Via Santa Maria, 46, I-56126 Pisa, Italy
email: salerno@iei.pi.cnr.it

Abstract-- A first-order Born approximation tomographic technique from far-field backscattering data, proposed and analyzed elsewhere, is first introduced. The data model adopted is linear, but the reconstruction algorithm is nonlinear, and its resolution power is not directly related to the working frequencies. Some simulated experimental results are then presented to evaluate the performance of the technique in the cases where the linear data model is not strictly justified.

I. INTRODUCTION

Microwave tomography is an interesting tool for nondestructive diagnosis of dielectric materials. However, rather expensive reconstruction algorithms derive from realistic (i.e. nonlinear) data models. The first-order Born approximation leads to a simple Fourier relationship between the measured data and the complex permittivity of the object under test. A Fourier reconstruction, however, yields highly ambiguous images, especially from data sets collected by a monostatic system. In [1] and [2], we suggested to adopt the first-order Born data model and a nonlinear reconstruction algorithm, the projected Landweber method [3], that avoids some of the problems related to linearization. This approach has advantages over the fully linear approaches, in that it yields better reconstructed images, and over the fully nonlinear approaches, in that it is much less expensive computationally.

For perfectly lossless objects, this algorithm yields quantitative images even in the cases where Fourier techniques would only achieve low-resolution or highly ambiguous images. To reconstruct the complex object function for lossy materials, a preprocessing strategy was proposed in [2]. This strategy, along with the projected Landweber method, was experimented in perfect Born conditions, and gave good results for both the real and imaginary parts of the object function. The next step in the validation of this technique is to test it with non-Born data. The key point to assess experimentally is the maximum allowed deviation from the first-order Born conditions that still permits the reconstruction of readable images. The algo-

rithm proposed in [1] for lossless objects is fairly robust against the distortions of the backscattered field with respect to the Fourier transform of the object function. The experimental evidence drawn from the preliminary tests presented here leads us to conclude that the algorithm for lossy objects is much less tolerant with respect to non-Born conditions if compared with the previous algorithm.

This paper is organized as follows. Section II briefly presents the simple multifrequency, far-field, monostatic measurement procedure and the reconstruction technique proposed in [2]. In Section III some experimental results from synthetic data calculated by a moment method [4] are shown. These results enable us to make the remarks reported in the concluding Section IV. All the details on the technique presented here and on previous experiments from real and simulated data can be found in [1] and [2], and in the references therein.

II. THE TOMOGRAPHIC TECHNIQUE

Figure 1 schematically shows the illumination-measurement system from which the backscattering data are collected. The object under test is placed on a rotating pedestal in the far-field zone of the antenna. The microwave source sends a signal at any frequency in the antenna bandwidth. The antenna illuminates the object, and receives the backscattered field. The complex envelope of the received signal is measured in amplitude and phase by the coherent receiver. Let us now introduce the notation used in this paper, directly assuming a two-dimensional

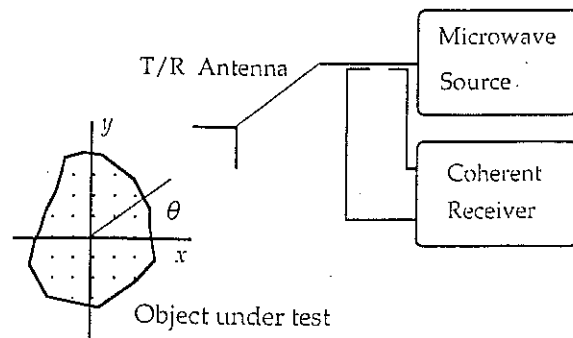


Fig. 1. Illumination-measurement system

geometry. The original 3D framework is described in [1]. The 2D dielectric contrast of the object under test is a complex function, whose imaginary part depends on the frequency, f , of the exploring radiation [2]:

$$g'(x,y) = \gamma(x,y) - \frac{j}{f} \xi(x,y), \quad (1)$$

where γ and ξ are real positive functions, related to the relative permittivity and the conductivity of the object, respectively. Let us assume that the conditions to apply the first-order Born approximation are perfectly satisfied. If the backscattered field is measured for all the incidence angles θ between 0 and 2π , and for all frequencies in a certain passband $f_{min}-f_{max}$, the data set available will be a sampled version of the following function:

$$W(f,\theta) = \Gamma(-\rho \sin \theta, -\rho \cos \theta) - \frac{j}{f} \Xi(-\rho \sin \theta, -\rho \cos \theta), \quad (2)$$

where Γ and Ξ are the Fourier transforms of γ and ξ , respectively, and $\rho=2f/c$, c being the velocity of light in the medium where the object under test is immersed. A strategy to eliminate f from Equation (2) is suggested in [2]. This strategy leads to the definition of a new object function, $g=\gamma+j\xi$. The data function W is modified as follows:

$$\begin{aligned} G_B(s_x, s_y) = & \\ = \Re & \frac{W(f,\theta) + W(f,\theta+\pi)}{2} + j \Re \frac{W(f,\theta) - W(f,\theta+\pi)}{2j} + \\ -j f \Im & \frac{W(f,\theta) + W(f,\theta+\pi)}{2} + f \Im \frac{W(f,\theta) - W(f,\theta+\pi)}{2j}, \end{aligned}$$

$$\text{with } s_x = -\rho \sin \theta, \text{ and } s_y = -\rho \cos \theta. \quad (3)$$

Symbols \Re and \Im denote real and imaginary parts, respectively. It can be shown that G_B is related to g through the following operatorial equation

$$G_B(s_x, s_y) = T_B \text{FT}_D g(x,y) \quad (4)$$

where T_D is a space limiting operator that sets to zero any function outside a domain D entirely containing the object under test, F is the Fourier transform operator, and T_B is a band limiting operator that sets to zero any function outside the annulus centered in the origin of the Fourier plane, with inner and outer radii $\rho_{min}=2f_{min}/c$ and $\rho_{max}=2f_{max}/c$, respectively. The tomographic

reconstruction problem consists in solving Equation (4) from knowledge of B , D and G_B . The reconstruction algorithm adopted in [2] is the iterative projected Landweber method, whose scheme is in this case

$$\begin{aligned} g_{n+1} = \sup \left\{ \Re \left[g_n + \tau T_D (F^{-1} G_B - F^{-1} T_B F g_n) \right], 0 \right\} + \\ + j \sup \left\{ \Im \left[g_n + \tau T_D (F^{-1} G_B - F^{-1} T_B F g_n) \right], 0 \right\}, \end{aligned} \quad (5)$$

with an initial guess, g_n , equal to zero everywhere, and a relaxation parameter, τ , chosen within an appropriate interval [3].

The validity of the preprocessing formula (3) can easily be verified by exploiting (1), (2) and the reality of functions γ and ξ , which implies that Γ and Ξ are Hermitian symmetric. However, if the Born approximation is not strictly justified, Equations (2) and (4) do not hold true, and thus the iterative procedure (5) is not valid anymore. It is to note that the Born conditions can be enforced by suitably tuning the working frequencies of the measurement system; on the other hand, it is interesting to see to what extent Procedure (5) can give useful results in non perfect Born conditions. Indeed, unlike the Fourier reconstruction techniques, the algorithm presented here has a resolution power that does not depend directly on the frequencies adopted, thus, lowering the frequency values do not necessarily imply a loss of resolution. The presence of distortion and noise, however, limits the resolving power achievable, and this makes interesting to know the allowed deviation from the Born conditions.

The algorithm proposed in [1], which does not consider the imaginary part of the contrast, is able to yield useful qualitative images even with considerable mismatches between the object and the background medium. This insensitivity to nonideal conditions is still to be demonstrated for the algorithm presented here. The procedure implemented by Equations (3) and (5) has been experimented with perfect Born data and with real measurements on very low-loss objects, giving encouraging results [2]. In Section III, we report the first results obtained by using a moment-method simulation code to generate the data sets to be processed.

III. EXPERIMENTAL RESULTS

To test the real feasibility of the method described above, we designed a synthetic phantom, whose shape is shown in Figure 2a. From this 2D structure, we calculated the backscattered field for a sufficient number of incidence angles and working frequencies, assuming a uni-

form, plane-wave incident field. After discretizing the phantom in square cells with edges of about 0.94 cm, the simulated backscattered data were obtained through the moment-method algorithm introduced in [4]. These data were then input to the reconstruction procedure, and the quality of the resulting images was evaluated.

The permittivity and the conductivity of each discretization cell can be set at any value within the range allowed by the simulation code. For these first experiments, however, we only chose to assign two values to these quantities, one for the black region and one for the shaded region shown in Figure 2a. In any case, we assumed that the body is immersed in air, that the D domain (see discussion after Equation 4) is a circle with a diameter of 22 cm, that 10 iterations of Scheme (5) are performed, and that the relaxation parameter τ is fixed at 1. As a first illustration of the method, we show the difference between the Fourier and the Landweber reconstructions in a case where the Born conditions are not satisfied. We assumed a uniform relative permittivity $\epsilon=1.8$ and a uniformly zero conductivity. In Figure 2b, the Fourier reconstruction, with frequencies ranging from 1.5 GHz to 3 GHz is shown. A Landweber reconstruction of the same object is shown in Figure 2c. It is easy to observe that the second image has less artifacts than the Fourier reconstruction, but some distortions still remain, since the object is too mismatched with respect to the background. Just for comparison, in Figure 2d we show the Landweber reconstruction on a data set obtained from measurements in the range 1-2 GHz. In this case we are closer to Born conditions, and the image has less artifacts if compared to the previous one. However, the resolution is slightly worsened.

In the next example, we use again the working passband between 1.5 and 3 GHz, and give the phantom a uniform relative permittivity $\epsilon=1.1$, and a conductivity $\sigma=0.001 \Omega^{-1}\text{m}^{-1}$ in the black region and $\sigma=0.01 \Omega^{-1}\text{m}^{-1}$ in the shaded region. The results, for real and imaginary parts are shown in Figure 3. It can be seen that the shape of the phantom has been reconstructed fairly well, and, in the imaginary part, the spot with higher conductivity can be clearly distinguished from the rest of the object.

To test the capability of discriminating different conductivity values in non-Born conditions, we tried to reconstruct the phantom with the same conductivity values as before and a relative permittivity $\epsilon=1.5$. The result is shown in Figure 4. Let us observe that the imaginary part should be the similar to the one in Figure 3b, but

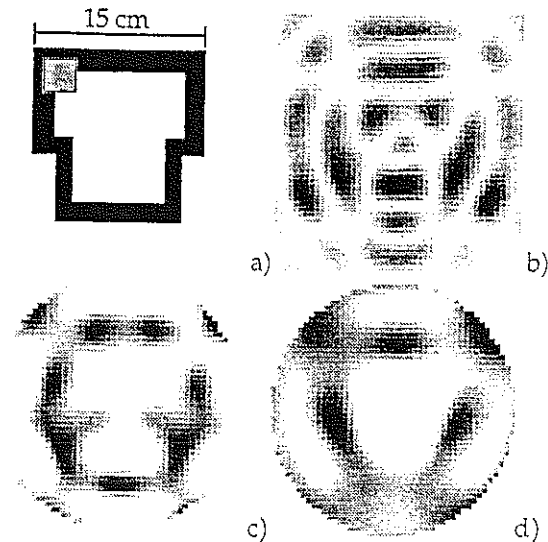


Fig. 2. a) Synthetic phantom used for the numerical simulations. b) Fourier reconstruction, $\epsilon=1.8$, $\sigma=0$, frequency range 1.5-3.0 GHz. c) Landweber reconstruction, frequency range 1.5-3.0 GHz. d) Landweber reconstruction, frequency range 1.0-2.0 GHz.

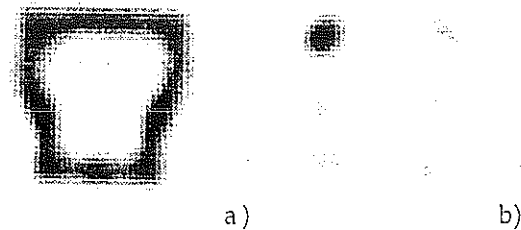


Fig. 3. Landweber reconstruction of the phantom with $\epsilon=1.1$, $\sigma=0.001 \Omega^{-1}\text{m}^{-1}$ in the black region, and $\epsilon=1.1$, $\sigma=0.01 \Omega^{-1}\text{m}^{-1}$ in the shaded region. Frequency range 1.5-3.0 GHz. a) Real part. b) Imaginary part.

the higher mismatch in this case caused a degradation in the reconstructed image, especially as far as the fidelity in the relative values of the conductivity is concerned. The real part still shows a good agreement with the overall shape of the phantom and with the uniform permittivity value assumed, but it also shows a degradation with respect to the result in Figure 3a.

As a last example (Figure 5), we report the result obtained by fixing a uniform relative permittivity $\epsilon=1.5$, and multiplying the previous conductivity values by a factor of 10. In this case, the phantom shape can still be recognized, but the presence of the highly lossy spot degrades the reconstruction of the real part of the object function, where an erroneous white area appears in the upper left corner.

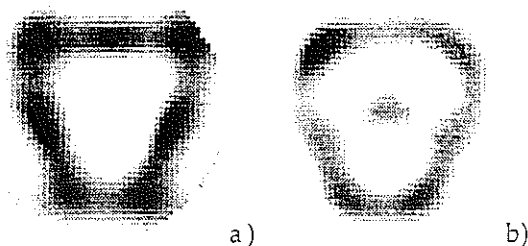


Fig. 4. Landweber reconstruction of the phantom with $\epsilon=1.5$, $\sigma=0.001 \Omega^{-1}\text{m}^{-1}$ in the black region, and $\epsilon=1.5$, $\sigma=0.01 \Omega^{-1}\text{m}^{-1}$ in the shaded region. Frequency range 1.5-3.0 GHz. a) Real part. b) Imaginary part.

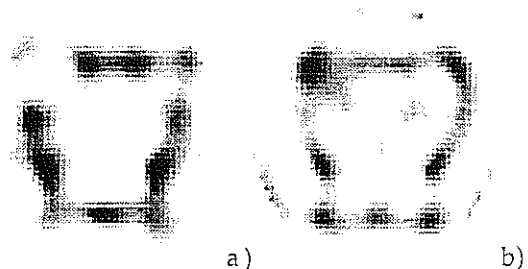


Fig. 5. Landweber reconstruction of the phantom with $\epsilon=1.5$, $\sigma=0.01 \Omega^{-1}\text{m}^{-1}$ in the black region, and $\epsilon=1.5$, $\sigma=0.1 \Omega^{-1}\text{m}^{-1}$ in the shaded region. Frequency range 1.5-3.0 GHz. a) Real part. b) Imaginary part.

IV. CONCLUDING REMARKS

In the linear tomographic reconstruction techniques based on the first-order Born approximation it is possible to extract Fourier data from the measured scattered field. If the measurements are not performed in Born conditions, some distortions are introduced in these Fourier data. This effect severely limits the usefulness of linear diffraction tomography.

The satisfaction of the Born conditions can be improved by lowering the working frequencies of the measurement system. By so doing, however, the passband of the Fourier data is reduced, and the spatial resolution of the reconstructed images is worsened proportionally to the reduction in the maximum frequency adopted. This drawback becomes important especially with large objects, even if their mismatches are not particularly strong.

Provided that a domain D , entirely containing the object function support is known, a strategy to partly recover the resolution lost by lowering the frequencies is to adopt a nonlinear reconstruction algorithm, such as the projected Landweber method described here.

The reconstruction of the imaginary part of the contrast function of a lossy object is another problem, arising when multifrequency data

have to be used, as in all the cases where a monostatic measurement system is available. In these cases, applying Equation (3) to the measured data eliminates the frequency dependence from the functions to be reconstructed, but only if the Born conditions are verified. Even a slight distortion in the Fourier data can produce very distorted reconstructed images. What is the maximum deviation allowed from the Born conditions is still to be found, however, we can say that the capability of getting a good image depends not only on the complex permittivity of the object under test, but also on its shape. Due to the passband limitations, a complicated shape should be more difficult to reconstruct than a simple one, even in the same mismatch conditions. For our purposes, an image can be considered complicated when it has considerable high spatial-frequency components.

The experimentation reported here should still be completed for a number of configurations, object function values, and frequency ranges adopted. Experiments from real measurements are also expected.

To draw a conclusion, at least on the basis of the particular results reported here, the Landweber method is able to extend the usefulness of Born approximation tomographic algorithms, but it also has its limits, caused by the low frequencies to be used with strongly scattering and/or very large objects. When these limits are exceeded, the only thing we can say so far is that more adequate data models must be used in devising the reconstruction algorithms. Appropriate data models, though scalar, should at least be nonlinear, and this implies using reconstruction algorithms that are normally very complicated and expensive computationally. For some examples of this kind of algorithms, the reader is referred to the bibliography in [1]. A major breakthrough in computing strategies and in hardware is needed to bring these techniques to real-world applications.

V. REFERENCES

- [1] E. Salerno, "Microwave Tomography for Compact-Support Dielectric Objects", *Int. J. of Imaging Systems and Technology*, Vol. 9, No. 1, pp. 14-23, 1998.
- [2] E. Salerno, "Microwave Tomography of Lossy Objects from Monostatic Measurements", *IEEE Trans. Microwave Theory and Techniques*, to appear
- [3] M. Piana, M. Bertero, "Projected Landweber Method and Preconditioning", *Inverse Problems*, Vol. 13, No. 2, pp. 441-463, 1997.
- [4] J.H. Richmond, "Scattering by a Dielectric Cylinder of Arbitrary Cross-Section Shape", *IEEE Trans. Antennas and Propagation*, Vol. 13, No. 3, pp. 334-341, 1965.